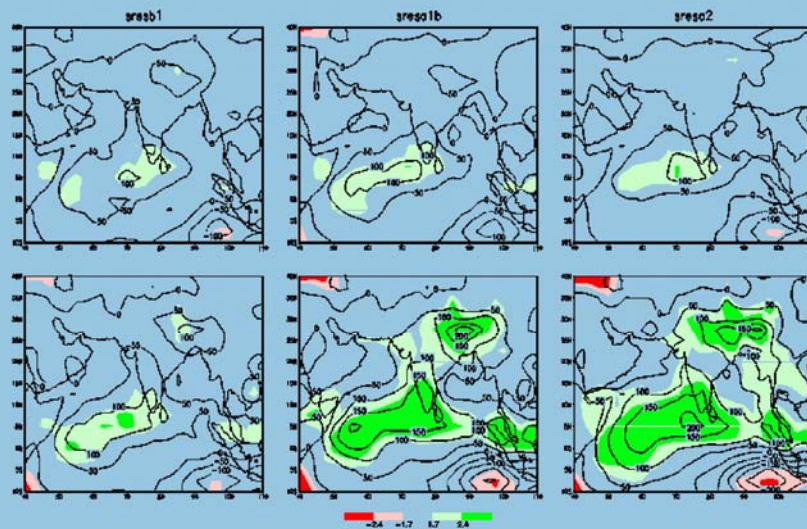# Examining Indian Monsoon Variability in Coupled Climate Model Simulations and Projections

Ashwini Kulkarni, RH Kripalani
and
SS Sabade

February 2010
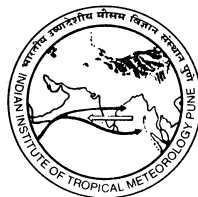
Indian Institute of Tropical Meteorology
Pune - 411 008, India

Examining Indian Monsoon Variability in Coupled Climate Model Simulations and Projections

Ashwini Kulkarni, R.H. Kripalani
and
S.S. Sabade

FEBRUARY 2010

Indian Institute of Tropical Meteorology

Dr. Homi Bhabha Road, Pashan Pune - 411 008
Maharashtra, India

E-mail : lip@tropmet.res.in   Fax : 91-020-25893825
Web : http://www.tropmet.res.in   Telephone : 91-020-25904200

CONTENTS

Examining Indian Monsoon Variability in
Coupled Climate Model Simulations and Projections

Ashwini Kulkarni, R.H. Kripalani and S.S. Sabade

ABSTRACT

South Asian summer monsoon (June through September) rainfall simulation and its potential future changes are evaluated in a multi-model ensemble of global coupled climate models outputs under World Climate Research Program Coupled Model Intercomparison Project (WCRP CMIP3) data set. The response of South Asian summer monsoon to a transient increase in future anthropogenic radiative forcing is investigated for two time slices , middle (2031-2050) and end of the 21st century (2081-2100) in the non-mitigated Special Report on Emission Scenarios (SRES) B1, A1B and A2 .There is large inter-model variability in simulation of spatial characteristics of seasonal monsoon precipitation. Ten out of 25 models are able to simulate space-time characteristics of South Asian monsoon precipitation reasonably well for the twentieth century.

The response of these selected 10 models have been examined for projected changes in seasonal monsoon rainfall. The multi-model ensemble of these 10 models project significant increase in monsoon precipitation with global warming. The substantial increase in precipitation is observed over western equatorial Indian Ocean and southern parts of India. However the monsoon circulation weakens significantly under all the three climate change experiments. Possible mechanisms for projected increase in precipitation have been discussed. The surface temperature over Asian landmass increases in pre-monsoon months due to global warming and heat low over north-west India intensifies. The dipole snow configuration over Eurasian continent strengthens in warmer atmosphere which is conducive for enhancement in precipitation over Indian landmass. No notable changes have been projected in the El Nino-Monsoon relationship which is useful for predicting interannual variations of the monsoon.

1. Introduction

World Climate Research Program / Climate Variability and Predictability (WCRP/CLIVAR) Working Group on Coupled Models (WGCM) organized an unprecedented international effort to run a coordinated set of twentieth and twenty-first-century climate simulations, as well as several climate change commitment experiments leading to the Fourth Assessment Report of Intergovernmental Panel on Climate Change (IPCC AR4). 25 modeling groups all over the world participated in this program and the model data were collected, archived and made available to the international climate community by Program for Climate Diagnosis and Inter-comparison (PCMDI), USA. These models are forced with concentrations of green house gases and other constituents derived from various emission scenarios ranging from non-mitigation scenarios to idealized long-term scenarios (Meehl et al 2007a).   There are three experiments, also known as storylines, B1, A1B and A2. Together they describe divergent futures that encompass a significant portion of the underlying uncertainties in the main driving forces. They cover a wide range of key "future" characteristics such as population growth, economic development, and technological change. The availability of such a large number of models provides considerable opportunity to assess the ability of these models to produce mean climate state of the present century as well as prudent projections of future climate change.

The South Asian sub-continent is highly vulnerable to climate variability/change due to its dense human population. Also its economy and agriculture mainly depends on monsoon rainfall. Over South Asia the summer is dominated by southwest monsoon which spans four months from June to September and dominates seasonal cycles of the climatic parameters. The behaviour and changes in monsoon precipitation play a vital role in economical progress of this region. Many of the coupled models have shown increase in precipitation over south Asia in warming climate (IPCC 2007; Christensen et al 2007). The confidence in regional precipitation projections may depend on how well the models are able to produce the 20th century monsoon rainfall. So it is necessary that to study the projections the models should simulate the present century climate reasonably well. One of the basic aims of IPCC AR4 model simulations is to assess the ability of the global coupled climate models to produce prudent projections of future climate change. To define the mean climate state we use the simulations from 20th century, a 20c3m experiment.

Model evaluations have been conducted as part of dedicated projects eg CMIP(Coupled Model Intercomparison Project : Meehl et al 2000; Covey et al 2003; Rao 2004), AMIP (Atmospheric Model Intercomparison Project : Gadgil and Sajani 1998; Gates et al 1999) and CLIVAR (Climate Variability and Predictability)/Monsoon GCM (General Circulation Model) Intercomparison Project(Kang et al 2002).

The second obvious aim of IPCC AR4 experiments is the generation of future projections. Almost all models show increase in precipitation and weakening of monsoon circulation in future projections (Chistensen et al 2007; Meehl et al 2007b). May (2004) has examined the potential impact of anticipated increase in green house gas

1

concentrations on different aspects of Indian summer monsoon in two time slices of ECHAM4 AGCM. He has shown that intensification of monsoon rainfall over Indian region is related to intensification of atmospheric moisture transport into this region. Ueda et al (2006) have examined the projected changes in Asian monsoon precipitation by using multi-model ensemble of 8 models. They have shown the intensified monsoon rainfall over India with weakening of monsoonal flow in Special Report on Emission Scenarios (SRES) A1B experiment. Kripalani et al (2007a) have extensively analyzed the model outputs of 22 models from WCRP CMIP3 dataset for the twentieth century simulations to study the ability of models to simulate present climate over south Asian region. They have examined the temporal features of the seasonal monsoon precipitation time series. Ten out of 22 models could simulate the monsoon rainfall over South Asian domain reasonably well. They have also analyzed the characteristics of climate change projections in the experiment 1% per year CO_2 increase to doubling at year 70, simulated by these ten models. This experiment give standard metric to assess the coupled transient response. The future projections over South Asian domain are examined in three twenty-first century climate change simulations from 2000 to 2100 (i) SRES B1 (low forcing ie. CO_2 concentration about 550 ppm by 2100); (ii) SRES A1B (medium forcing ie. CO_2 concentration of about 700 ppm by 2100) and (iii) SRES A2 (high forcing ie. CO_2 concentration about 820 ppm by 2100). In the middle of the 21st century scenarios A1B and A2 have similar CO_2 concentrations and B1 has somewhat less concentration as compares to these two. The increase in CO_2 concentration is not very sharp in this period. However at the end of the 21st century (2081-2100) the three scenarios divert a lot. Scenario A2 has rapid increase. A1B exhibits much slow increase in CO_2 as compared to A2. B1 has almost stable and minimum concentration of CO_2 (for details please refer to Meehl et al 2007b).

In order to study the projections we apply the technique of multi-model ensemble (MME). MME is defined as average of simulation results from multiple models. The reason to focus on MME is that averages across structurally different models empirically show better large scale agreement with observations. The extended use of MME of projections of future climate change therefore provides higher quality and more consistent climate change information. The use of MME has been shown in other modeling applications to produce simulated climate features that has improved over single models alone (Christensen et al, 2007; Meehl et al 2007b). The method has been applied to model evaluation or estimation of the climatology from coupled atmosphere-ocean GCMs (AOGCMs) (McAvaney et al 2001), climate change projection from AOGCMs (Cubasch et al 2001; Giorgi and Mearns 2002), and climate change detection from AOGCMs (Gillett et al 2002). Kripalani et al (2007b) have applied MME technique to study response of the East Asian summer monsoon to doubled atmospheric CO_2. In the present study MME of ten selected models is used over South Asian region to study the projections in 21st century in SRESB1, SRESA1B and SRESA2 experiments. The simulated changes in seasonal precipitation and the associated circulation are documented for two time slices, one in the middle of 21nd century, (2031–50) and the other at the end of the 21nd century (2081–2100) relative to 1981–2000 in the 20th century.

Section 2 describes the data used in this analysis. In section 3 the models are evaluated with respect to their similarity with observed seasonal mean rainfall pattern. The projections of these models are discussed in section 4. The possible mechanisms for projected changes in precipitation are described in section 5. Section 6 describes the simulation and projected changes in ENSO-Monsoon and IOD-Monsoon relationships and finally the results are summarized in section 7.

2. Data sets used

(i)   25 atmosphere-ocean general circulation modeling (AOGCMs) groups have participated in IPCC AR4 coordinated experiments. The IPCC standard outputs from 22 coupled GCMs are available and archived by the WGCM (Working Group on Coupled Models) Climate simulation panel and the Program for Climate Model Diagnosis and Inter-comparison (PCMDI) at the Lawrence Livermore National Laboratory, USA. For status of the IPCC database, model documentation, related references etc. one can visit the website http://www-pcmdi.llnl.gov/ipcc/info_for_analysts.php. The IPCC identifications, the modeling groups and the key references are given in Table 1. There is a fairly large range in the horizontal resolution of the models varying from 1.125^0 long / lat to 5^0 long by 4^0 lat. Since ensemble averaging reduces the noise level in model-simulated quantities especially on regional and smaller scales, averages based on all the available runs are also prepared for each model. Thus uncertainties could be reduced by using results from ensemble averages. Most of the results presented are based on ensemble averaging. All the information about model resolutions, data length for '20c3m' run, convection schemes and flux corrections have been given in Table2.

(ii)   The model simulated sea level pressure, vector wind patterns and sea surface temperatures are compared to NCEP–NCAR (National Centre for Environmental Prediction–National Center for Atmospheric Research: Kalnay et al., 1996) Reanalysis data.

(iii)   The Climate Prediction Center Merged Analysis Precipitation (CMAP; Xie and Arkin 1997). The CMAP precipitation analysis (obtained from the website ftp://ftpprd.ncep.noaa.gov), which has a resolution of 2.5^0 lat by 2.5^0 long, was formed by combining rain gauge measurements with several types of satellite data and the NCEP-NCAR reanalysis data (Kalnay et al 1996). The different data sources were weighted with their expected, geographically varying relative accuracy. In practice, gauge measurements have the highest weight where they are available (Xie and Arkin 1997)

(iv)   Future projections of precipitation flux over South Asian domain are downloaded in three twenty-first century climate change simulations SRES B1, A1B and A2 from 2000 to 2100. The projected changes in precipitation are examined   in two time slices, middle of the century 2031-2050 and at the end of the century 2081-2100.

(v)   To understand the possible mechanisms for projected changes in precipitation air pressure at sea level, surface temperature, snow fall flux, surface vector winds and atmospheric water vapor content outputs for the three SRES experiments are also downloaded.

(vi)   Time series of seasonal precipitation (at www.tropmet.res.in) derived from station data of the India Meteorological Department (IMD), designated as Indian summer monsoon rainfall (ISMR). This series excludes rainfall data over the northeast hilly regions. This series, available since 1871 has been widely used as a measure to express quantitatively the inter-annual monsoon variability. The mean ISMR is 851.4 mm with a standard deviation of 82.4 mm. The variation of this series has been widely studied and can be considered as a measure of the intensity of monsoon over the Indian region.

3. Evaluation of Models

One of the highest priority output field is the precipitation flux. The monthly data for this variable for all the models and all the available runs (based on different initial conditions) under '20c3m' scenario have been downloaded. Typically modeling groups run a "pre-industrial control" run which is a long control with pre-industrial conditions (CO_2 concentrations from that time etc.) Then the 20th century runs start from different times in the control run, usually separated by at least 20 or so years. This will provide different initial state in the coupled system for different 20th century runs . From these data sets the following products are prepared

  (a)   Monthly average rainfall in mm/month for the South Asian Region (5-35 N, 65-95 E) to examine the annual cycle

  (b)   Seasonal (June through September : JJAS) average rainfall in mm over South Asian region to investigate the spatial mean and variability patterns

  (c)   Time series of seasonal rainfall for South Asian domain as a whole for all the available years to examine the inter-annual summer monsoon rainfall variability, long-term trends and the biennial tendency.

3.1   Observed and simulated Annual cycles

Since the model simulations are most stable over the period 1981-2000, the simulated as well as observed annual cycle is based on this data period. The CMAP average precipitation (mm) for each month, depicting the observed annual cycle, is shown in each panel of Fig. 1. Over the course of the annual cycle precipitation changes from less than 50mm/month during the January–April period to more than 200mm/month during the peak summer monsoon period of June–August. Thus the annual cycle is characterized by a sharp increase from April to June and thereafter a gradual decrease from September. An examination of the model simulations (Fig. 1) suggests that they can be classified into the following broad categories: (i) Seven models (bccr, ccsm, cgcm, cnrm,echam, gfdl1 and mirocm: Fig. 1 upper left panel) simulate a similar annual cycle in terms of shape and magnitude to observed characteristics. However, cnrm simulates excess precipitation during November–December. (ii) Six models (echo, gissh, gissr, inmcm, mriand ukmog: Fig. 1 upper right panel) simulate the shape of the annual cycle well but underestimate precipitation amounts, in particular during spring and summer periods (iii) Six models

4

(csiro, fgoal, gfdl0, gissa, miroch and ukmoc: Fig.1 lower left panel) simulate peak rainfall a month later than observed, resulting in the underestimation of rainfall during spring and summer. (iv) Three models (bccc, ipsl and pcm: Fig. 1 lower right panel) are unable to simulate the annual cycle accurately. While model pcm depicts two peaks, model bccc is unable to simulate even the summer monsoon season. In the subsequent analysis, only those models falling in the first three categories are retained, since these are considered to realistically simulate maximum rainfall during the south Asian summer monsoon period (JJAS)

3.2   *Inter-annual variability*

The time series of observed monsoon rainfall has some well known inter-annual characteristics such as random fluctuations with no long-term trend, a coefficient of variation (CV) of about 9%, and a tendency for biennial oscillation. A simple way to ascertain the biennial tendency is to compute the lag-1 autocorrelation A negative (positive) value of the lag-1 autocorrelation would indicate the presence (absence) of the biennial oscillation. Long-term changes ie. trend are examined with the Mann-Kendall rank statistic. Based on CMAP (IMD) data for the 1981–2000 period, mean summer monsoon rainfall is 798 (840) mm and CV is 8.6 (9.0)%. The value of the Mann-Kendall statistic (lag-1 autocorrelation) based on 130 years of IMR data is -0.01 (-0.10), suggesting no significant long-term trend and the presence of biennial tendency. Since the CMAP data are available for a short period, the trend is not calculated. However, the lag-1 autocorrelation for the available CMAP data is -0.28. The performance of the models in simulating the inter-annual variability is judged with respect to the mean monsoon rainfall, CV, trend and the lag-1 autocorrelation. Long-term trends and the lag-1 autocorrelations are based on all available data (~150 years) for each model under the '20c3m' experiments. A scatter plot of the mean seasonal rainfall and the CV for the 22 models is shown in Fig. 2. The spread of the models suggests the diverse nature of the model simulations. While the mean rainfall varies from 501mm (csiro) to 907mm (miroch), CV varies from 2.9% (gissr) to 13.1% (csiro). In general, most of the models simulated the dry bias in the total seasonal precipitation. A similar scatter plot for trend and biennial tendency is shown in Fig. 3. Six models (fgoal, gfdl0, gfdl1, gissa, gissh and ukmog) simulate significant negative trends while one model (ccsm) simulates a significant positive trend. These regional trends could be due to the internal variability within a model and could imply a bias that distorts future projections. Out of the remaining 12 models (showing no long term trends), the biennial tendency is captured well by eight models (those lying between horizontal lines B and C and left of vertical dashed line A: Fig. 2). Based on the scatter plots in Figs. 2 and 3, seven models (bccr, cgcm, cnrm, echam, miroch, mirocm and ukmoc: marked in the rectangular box in Fig. 2) are considered to simulate the inter-annual summer monsoon mean and variability well. Though echam does not simulate the biennial tendency, it is retained since other characteristics such as the mean rainfall, coefficient of variation and long-term trend are well simulated.

3.3   Spatial Patterns

The simulation of the rainfall patterns over Indian region has been proved to be a difficult task due to its extremely complex spatial distribution and large precipitation gradients. This may pose difficulties in replicating the exact pattern with the correct amplitude. Since the model resolutions vary substantially the areas of maximum / minimum precipitation and their amplitudes may show some shifts in these areas. The major observed features of the Indian summer monsoon rainfall are primary continental rain belt extending from the Bay of Bengal across the Indo-Gangetic plains corresponding to the monsoon trough and the low pressure systems ; secondary oceanic rain-belt near the equatorial regions around 5^0 S ; west coast rainfall maximum due to the western ghats orographic barrier; maximum rainfall over northeast India associated with the Himalayan orography; low rainfall over northwest India and the southeast peninsula. We have examined the seasonal rainfall pattern simulated by all 25 models, only 10 models which could capture the temporal characteristics reasonably well, were able to simulate the above spatial features also.

3.4   Taylor diagram

To examine the spatial resemblance of the simulated and observed patterns we represent them in Taylor diagram. Taylor diagram (Taylor 2001) is a graphical summary of how closely a set of patterns matches observations. The similarity between two patterns is quantified in terms of their correlations, their centered root mean square error and the amplitude of their variations (represented by their standard deviations). Fig 4 represents the Taylor diagram analysis for the precipitation of South Asian region. In the Taylor diagram the radial distance from the origin represents the standard deviation ratio of the model simulated pattern with reference (CMAP) pattern. The pattern correlation between two fields is given by the azimuthal position and the normalized centered RMSE of the simulated pattern is given by the distance from the reference point of observations.

The selection of 10 models (highlighted models in Table 1) seem to be the best selection for true representation of spatial pattern of precipitation which has maximum pattern correlation, minimum RMSE and negligible bias. The spatial rainfall distribution based on CMAP and the ten selected models as well as their multi-model ensemble (MME) is shown in Fig.5. MME of these 10 models reasonably captures all the spatial characteristics of seasonal monsoon over South Asian region. Hence we consider MME of these 10 models in further analysis.

4   Projected changes under Climate Change Experiments

The important aim of IPCC AR4 experiments is the generation of future projections. Almost all models show increase in precipitation and weakening of monsoon circulation in future projections (Chistensen et al 2007). The models which are not able to capture the characteristic spatial features of South Asian precipitation are not considered for their projections since the projected changes in monsoon precipitation by the models which fail to simulate the monsoon in 20th century may not have any merits.

In the present study MME of ten selected models is used over South Asian region to study the projections in 21st century in SRESB1, SRESA1B and SRESA2 experiments. To apply MME, each model has been interpolated on the uniform grid of 2.5^o lat/lon.

The projected changes in seasonal precipitation and the associated circulation are documented for two time slices, one in the middle of 21nd century, 2031–50 and the other at the end of the 21nd century 2081–2100 relative to 1981–2000 in the 20th century.

4.1   *Projected Annual Cycle : Precipitation*

To examine the nature of annual cycle in warming climate, the monthly average rainfall over south Asian domain under the three scenarios is examined. Fig 6 shows the monthly average of MME for 20th century (1981-2000) and the three climate change experiments (2081-2100). The annual cycle does not change much in the middle of the century 2031-2050. It is observed that the overall shape of annual cycle and the seasonal march would not change in future scenarios implying that the monsoon season will remain the same June through September with peak rainfall in July-August. Under scenario A1B the increase is 0.5 mm/day, while under B1approximately 1mm/day. A2 shows maximum increase of almost 1.5 mm/day. The MME projects a decrease of rainfall during winter and early spring (January through May) and increase in summer (June through August) and the following autumn (September through November), possibly indicating the extension /lengthening of summer monsoon rainfall period.

4.2   *Inter-annual variability*

The century long time series for seasonal rainfall has been prepared by averaging the rainfall over all grids in the south Asian domain under the 20C3m (1901-2000) and for the three scenarios (2001-2100).

Fig 7 depicts the 11-year running average of the MME time series of seasonal monsoon rainfall for 20c3m and for three climate change scenarios. It is very well observed that the simulated time series is highly random, however the time series under climate change scenarios do exhibit significant long term trends. The series under scenario A2 exhibit maximum increasing linear trend of 1.2 mm/year in seasonal rainfall. In scenario A2 there is rapid growth of   greenhouse gases   which will lead to more warming of the atmosphere and increase in   moisture, but it also specifies the somewhat greater sulphate aerosol concentration which may have cooling effect on the surface temperature and hence a slight weakening of monsoon precipitation. Hence though A2 has maximum concentration of CO2, the summer rainfall is less than that under A1B scenario.

4.3   *Projected changes in Precipitation patterns*

The change in seasonal monsoon rainfall in two time slices 2031-2050 and 2081-2100 with respect to the 20 years period 1981-2000 in 20th century run (20c3m)

has been examined. The rainfall increases substantially over certain regions. The significance of the difference has been tested by applying student's t test at each grid point. Fig 8 depicts the MME spatial patterns of the change in precipitation under the three SRES scenarios. The contours represent the magnitude of change in seasonal rainfall while the shading gives the t values of significant difference at 1% and 5% level.

In both the time slices under scenario B1, the precipitation is increased over south Asian region, however the change is significant only over southern tip of India and south equatorial Indian Ocean. Under A1B, area with significant increase expands. At the end of the 21st century the rainfall shows significant increase over entire Indian land region except north-west India. Also over Indian Ocean, the region expands to eastern Indian Ocean. However in south-eastern Indian Ocean along Sumatra coast the rainfall is substantially reduced. Under the scenario A1B slight reduction in rainfall amount is observed over the region south of 15° N. Under the scenario A2, scenario with maximum concentration of CO2, the increase in rainfall is significant over equatorial Indian Ocean in the middle of the 21st century. The rainfall is reduced over head Bay and north-eastern parts of India. This is the most recurring pattern of Indian monsoon rainfall (Kulkarni et al 1992). The north-east region is out-of-phase with the entire landmass. At the end of the century it shows a typical feature, a significant decrease in rainfall over north-eastern India, Himalayan-Tibetan region while there is substantial increase over the region south of 20°N and entire equatorial Indian Ocean basin. Along the monsoon trough region, the east-west region from north-west India to head Bay of Bengal, the rainfall does not show significant change. The dry conditions north of monsoon trough region imply strong monsoon over the region south of trough region which implies that in future south Asian region, especially India will receive more rainfall than that in 20th century.

5   Possible mechanisms for increase in mean precipitation

The land-sea temperature contrast is the basic forcing mechanism of the south Asian summer monsoon. The other precursors to Indian monsoon involve snow fall during previous winter and spring, El Nino Southern Oscillation (ENSO) phenomenon over the Pacific, heat low over Pakistan and northwest India etc. Strong temperature gradient between equatorial Indian ocean and Northwest India is conducive for strong monsoon activity over India. The persistence of deep snow and the greater aerial extent of snow cover in winter/spring could be an important factor in determining the slower and weaker build-up of the summer season, continental heat sources and subsequent monsoon strength. This is well supported by the inverse relationship between snow cover and monsoon rainfall well documented in many publications employing dynamical and empirical approaches since the time of Blanford, over a century ago. To study the possible mechanisms for an increase in precipitation under the three scenarios, changes in winter snow cover, sea level pressure (slp) and surface temperature in May (pre-monsoon season), circulation and water vapour in the atmosphere during monsoon season are examined in two time slices, 2031-2050 and 2081-2100 with respect to 1981-2000 of 20th century runs.(Sabade et al , 2009)

5.1 Heat low over north India

The changes in sea level pressure (slp) in May for MME are presented in Fig 9. Top three panels show changes in May slp in the middle of the 21st century for three scenarios. In A1B the pressure has been substantially reduced over northwestern India extending upto Persia implying the strengthening of heat low. The pressure is also reduced over western Indian Ocean, The slp increases over northeastern region and the difference is statistically significant. In B1 similar pattern is observed. However in A2, in the middle of the 21st century the region of negative difference reduces a lot and positive difference is observed almost over the entire country. In the middle of the century the reduction in slp is not significant. At the end of the 21st century (Fig 9 bottom panel) , the significant reduction in slp is observed over heat low region over north-west India and western Indian Ocean in warmer climate, which may supply moisture to the cross equatorial flow from western Indian ocean to Indian landmass. The increase in pressure over northeastern region is maximum in A2 scenario. In B1 the region of positive difference is much smaller. Also the strengthening of heat low is not significant in B1. Thus in general, the heat low over northwest India and Persia and the establishment of the trough of low pressure over Indo-Gangetic plains are projected to intensify in the warming world. This feature is conducive to oceanic moisture convergence over landmass of India, leading to the enhancement of the mean summer monsoon precipitation. In all scenarios, in both time slices the pressure over Bay of Bengal shows increase of the order of 0.25 hPa which implies cooling over Bay of Bengal . This may result into reduction in development of low pressure systems and cyclones over Bay of Bengal. Also pressure over north-east India and foothills of Himalaya shows significant increase, implying weakening of monsoon over this region.

5.2 Monsoon Circulation

It is well known fact that precipitation is affected by strength of the monsoonal flows and amount of water vapor transported. Monsoonal flows and tropical large-scale circulations weaken in global warming scenario. There is emerging consensus that the effect of enhanced moisture convergence in a warmer, moister atmosphere dominates over any such weakening of circulation resulting in increased monsoonal precipitation. The dominant features of the strong monsoon circulation over south Asian region are the cross equatorial flow from Southern Hemisphere along the east coast of Africa, southwesterly/ westerly flow over the Arabian Sea, Indian peninsula and Bay of Bengal; development of low pressure area from northwest India to head Bay of Bengal, known as monsoon trough, with westerlies to its south and south-easterlies to its north. These features are well captured by all these models (Kripalani et al 2007). The projected changes in vector winds at 850 hPa for the season JJAS are shown in Fig 10. The shading is for significant difference at 5 and 1% levels. The upper panel shows change in circulation in the middle of 21st century while the lower panel at the end. The anomalous northeasterly/easterly

flow over Indian subcontinent (equator-10° N, 50°-100° E) implies the weakening of monsoon circulation in all scenarios. The weakening is comparatively less in scenario A2. The precipitation-wind paradox observed by Ueda et al (2006) for projected changes under scenario A1B is also observed under B1 and A2 experiments. This circulation pattern suggests warmer west Indian Ocean and comparatively cooler eastern Indian Ocean, possibly suggesting the development of positive Indian Ocean Dipole mode. However the southerly/southwesterly flow penetrating to Arabia, Pakistan region (10°-25° N, 50°-60° E) implies the possible shift in monsoon circulation. . In the middle of the 21st century the change in circulation is significant in Northern Hemisphere only. At the end of the century the circulation weakens significantly in Southern Hemisphere also which suggests that at the end of the century the cross equatorial flow itself is weakening.   The anomalous easterly flow in these projections over Bay of Bengal may be conducive for transport of oceanic moisture towards southern parts of India and Sri Lanka. An anomalous anti-cyclonic circulation is also noted over Bay of Bengal which may hinder the formation and development of low pressure systems and depressions over this region. In all the scenarios the weakening in monsoon circulation is not significant north of 20° N. Hence the northern parts of the country may not face significant change in monsoon circulation in 21st century.

5.3   *Eurasian snow cover*

Eurasian snow is one of the most vital predictor of seasonal rainfall over India. Kripalani and Kulkarni (1999) have shown that reduced snow over western Eurasia (20°-70° E) and enhanced snow over Eastern Eurasia (70°-140° E) during preceding winter is conducive for strong monsoon activity over India. Hence to examine whether snow cover plays any role in enhancement of precipitation in warmer climate, it is interesting to study the projected changes in snow cover in 21st century. Fig 11 depicts changes in snow cover under three scenarios in the middle and end of the 21st century in preceding winter season (December-January-February). In the middle of the century (upper panel) the snowfall over western Eurasia is projected to decrease by 10 to 40 mm in scenarios A1B and A2. In B1 also the reduction is projected but of the magnitude of around 10 mm. the snow is projected to increase over eastern Eurasia north of 70°N. No significant change is projected over Tibetan region in the middle of the century. At the end of the 21st century, much larger region shows decrease or increase in snow. In all the scenarios a substantial increase of 10 to 30 mm is projected over Tibetan region at the end of the 21st century. The snow is increased over western Eurasia and decreased over eastern Eurasia over much larger region.

Hence reduction in snow over western Eurasia and enhancement over eastern Eurasia strengthens the east-west dipole configuration over Eurasian region which is conducive for strong monsoon activity over Indian landmass in following summer.

5.4   Atmospheric water vapor

The increase in mean precipitation in the 21st century has been attributed to increase in water content of the atmosphere in warming climate   To assess this issue we determined the percent increase in precipitable water in JJAS (atmospheric water vapor content vertically integrated through the atmospheric column) projected in MME in the middle and at the end of 21st century in three scenarios. Fig 12 shows these MME patterns. In the middle of the century maximum increase in precipitatble water is of the order of 10% over Indian landmass. Since the variability of water vapour is very less, the t value is very large and hence has not been plotted. The increase is significant over entire region. At the end of the 21st century (Fig 12, lower panels), the maximum increase in precipitable water is 20-25% (15%)over Indian landmass and adjoining oceanic regions and around 40-50% (20%) over Himalaya-Nepal region and west Asia in scenarios A1B and A2 (B1). Thus the increase in moisture content of the atmosphere may lead to enhanced precipitation over south Asian domain

6   ENSO-Monsoon and IOD-Monsoon Relationship

ENSO is one of the dominant factors which is responsible for earth's year-to-year climate variability. Though ENSO-Indian monsoon relationship is proved to be weakened in recent times (Kripalani and Kulkarni, 1997), in the historical records majority of the ENSO events have led to weak monsoon activity over India. We try to observe changes in ENSO-Monsoon relationship in warming climate. We first examine the ability of these 10 models to simulate the life cycle of ENSO. The life cycle is   the composite based on the strong El NINO events (standardized JJA NINO3.4 SST greater than 1.0) simulated by each model. Fig 13 shows the life cycle of ENSO simulated by 10 models, their MME and the observed life cycle. Sea Surface Temperatures (SSTs) over east equatorial Pacific start warming around April-May, peaks in winter around December and then start decaying. Thus the life cycle of a typical ENSO event is approximately two years. All the models except ccm and ukc are able to simulate the ENSO life cycle reasonably well. Model bcr simulates the shape but decays rapidly. MME simulates the peak phase of ENSO event quite reasonably though in developing and decaying phase it simulates a warm bias.

6.1   ENSO-Monsoon Relationship

 It is well known fact that the observed concurrent inverse relationship between ENSO and Indian summer monsoon has been weakened in recent years (Kripalani and Kulkarni, 1997; Krishna Kumar, 1999). To examine whether the models also simulate the weakening of ENSO-Monsoon relationship in recent years we computed monthly correlations of SSTs over NINO3.4 region and the seasonal monsoon rainfall simulated by ten models in the 20th century. Fig 14 shows these correlations in two time slices 1961-1980 (solid line) and 1981-2000 (dashed line). The models cnr, ech, mih, mim show slight strengthening relationship. Remaining models   show that the relationship has not only weakened but even changed the sign (becomes positive) in recent 20 years.

11

To further study the projected changes in this relationship we compute correlations between projected rainfall and projected monthly SSTs over NINO3.4 region in the period 2081-2100. Fig 15 shows these correlations projected by 10 models under experiments B1 (dotted lines), A1B (dashed lines) and A2 (dash-dot lines). For comparison we have also plotted the simulated relationships in 20th century (solid lines). It is well observed that under all scenarios concurrent relationship in JJAS is projected to weaken or remain stable as compared to that in 20th century. Under scenario A1B as well as A2, similar feature is observed. Under A1B, only ccm and ukc project the strengthening of relationship, however these two models fail to simulate the life cycle of ENSO (refer Fig 13). Under A2, bcr and ccm project slightly stronger relationship than that in 20th century. Thus no clear conclusion can be drawn about projected changes in ENSO-Monsoon relationship. Hence ENSO forcing may not play any role in strengthening of seasonal monsoon rainfall over south Asian region. Also since there is lot of inter-model variability in these projected relationships, MME will not lead to any reasonable conclusion.

6.2   *IOD-Monsoon Relationship*

Recent studies   have pointed out that the Indian Ocean gives birth to a unique coupled ocean atmosphere mode, which may induce unusual rainfall distribution not only in the surrounding areas but other parts of globe also   This mode is termed as Indian Ocean Dipole Mode (IODM: Saji et al, 1999) in recent literature.

An index to quantify the IODM has been proposed by Saji et al (1999). This is the difference in SST anomaly between the tropical western IO (50° –70° E, 10° S–10° N) and the tropical southeast IO (90° –110° E, 10° S-Equator) and is denoted as Dipole Mode Index (DMI). The relationships found in earlier studies were between rainfall and SSTs spread over the IO. With the introduction of the term IODM, SSTs over the western and southeast IO have become the main focus of interest. While some studies report positive relation between IODM and monsoon rainfall over India, some report weak and insignificant relationship over the Asian monsoon domain.   Thus the relationship of the IODM with monsoon rainfall is still not clear. In fact a recent study (Kripalani et al, 2005) reports a stronger relationship with monsoon over East Asia than over South Asia. Since main Indian monsoon peaks in boreal summer, June through September and IODM starts developing in summer and peaks in autumn, it is logical to examine the influence of the monsoon on the dipole. Kulkarni et al (2007) have examined the association between extreme Indian monsoons and the dipole mode and they have shown that the relationship between DMI and IMR is strong following the monsoon. Also strong (excess) Indian monsoon damps the dipole mode over Indian Ocean.

Saji et al (2006) have analysed outputs of 17 coupled climate models from IPCC AR4 to examine their ability to simulate basin-wide variability of Indian ocean circulation. They have shown that the models with reasonable strong ENSO variability are largely successful in simulating the delayed response in Indian ocean. Almost all models simulate warm SSTs that are nearly uniform east of 60° E within the range of 27.5-29.5^{o}C. All

models capture SST cooling and suppressed convection in west Africa. With a few exceptions mean winds are weak on the equator. As a result the thermocline is quite flat along the equator much as in observations. Overall the models show high skill in simulating zonal distribution of SST, thermocline depth and precipitation along equator. Fig 16 represents the observed and simulated correlations between the seasonal rainfall over South Asia and monthly DMI for two time slices 19061-1980 (black) and 1981-2000(red). As it is seen the observed correlation is maximum though not very strong, following the monsoon season. The maximum correlation is of the order of 0.3 in Aug-Sept-Oct and it is observed to be strengthened in recent 20 years. It is seen that except ccm and ccm2, all other models fail to capture this relationship. Many models even simulate negative relationship and also the relationship seems to be weakened in recent 2 decades. Thus though almost all models are able to simulate the basin-wide Indian Ocean variability with reasonable skill, they fail to capture the relationship with Indian monsoon, hence the projected changes in IOD-Monsoon relationship may not give correct picture.

7   Summary and Conclusions

Based on the recommendations of the Intergovernmental Panel on Climate Change Third Assessment Report (IPCC, 2001) climate modeling groups around the world have performed a comprehensive, systematic, well designed and well coordinated set of 20th and 21st century climate change experiments. The 20th century simulated summer monsoon (June through September: JJAS) precipitation over the south Asian domain (5°–35^oN, 65°–95° E) for all available models and runs are analyzed with respect to the annual cycle, the inter-annual variability and the spatial characteristics. These simulated features are compared with the observed features and the degree of inter-model agreement is determined. Based on the performance of the models in simulating the 20th century precipitation variability over south Asia, 10 models were selected to examine future precipitation projections under three climate change experiments SRES B1, A1B and A2. The main conclusions are

(i)   19 of the 22 climate models simulate the shape of the annual cycle well with maximum precipitation during the JJAS period, but with some deviations in the magnitude. While one model simulates two peaks, another is unable to simulate the summer monsoon season.

(ii)   While seven models show long-term trends, eight are able to simulate the biennial tendency of the Indian monsoon rainfall. 10 models (bccr, cgcm, cgcm2, cnrm, echam, echo-g, miroch, mirocm and ukmoc) simulate the space-time monsoon variability reasonably well. The MME of these 10 models are examined for projections of monsoon rainfall   under three climate change experiments SRES B1, A1B and A2 in two time slices in the 21st century, 2031-2050 and 2081-2100

(iii) The seasonal precipitation over South Asian domain is projected to increase in 21st century.

(iv) The intensification of heat low over northwest India, intensification of low pressure monsoon trough over Indo-Gangetic plane could be a possible reason for enhancement in mean precipitation amount in 21st century. Also the amount of snow over western (eastern) Eurasia is projected to increase (decrease) hence strengthening the dipole configuration over Eurasian region. This may imply the changes in mid-latitude circulation conducive for strong monsoon over south Asian domain

(v) The weakening relationship between ENSO and South Asian monsoon is well captured by these 10 models. The projected relationship may not change significantly in the 21st century.

(vi) Though all models simulate the basin-wide variability of Indian Ocean circulation reasonably well, they fail to capture the IOD-Monsoon relationship.

The three climate change experiments considered here together describe divergent futures of the underlying uncertainties in the main driving forces. They cover a wide range of key "future" characteristics such as population growth, economic development, and technological change. The rate of population growth as well as the economic and technological development is simply astonishing in today's world. Hence it is very important to have correct future climate projections under these scenarios, especially in the densely populated region of the world like South Asia.

REFERENCES

Christensen JH., Hewitson B, Busuioc A. Chen X, Gao I, Held R, Jones R, Kolli RK, Kwon W-T, Laprise R, Magaña Rueda L, Mearns L, Menéndez CG, Räisänen J, Rinke A, Sarr A , Whetton P (2007) Regional Climate Projections. In: *Climate Change 2007: The Physical Science Basis. Contribution of Working Group I to the Fourth Assessment Report of the Intergovernmental Panel on Climate Change* [Solomon, S., D. Qin, M. Manning, Z. Chen, M. Marquis, K.B. Averyt, M. Tignor and H.L. Miller (eds.)]. Cambridge UniversityPress, Cambridge, United Kingdom and New York, NY, USA.

Covey C, AchutaRao KM, Cubasch U, Jones P, Lambert SJ, Mann ME, Phillips TJ, Taylor KE (2003) An overview of results from the Coupled Model Intercomparison Project. Glob Planet Change 37: 103-133

Cubasch U, Meehl GA, Boer GJ, Stouffer RJ, Diz M, Noda A, Senior CA, Raper S, Yap KS, (2001)   Projections of future climate change, *Climate Change 2001 : The Scientific Basis.* Contribution of Working Group I to the Third assessment Report of the Intergovernmental Panel on Climate Change (Houghton et al eds), Cambridge University Press, UK, 944 pp

Gadgil S, Sajani S (1998) Monsoon precipitation in AMIP runs. Clim Dyn 14, 659-689

Gates WL, Boyle J, Covey C, Dease C, Doutruiaux C, Drach R, Fiorino M, Gleckler P, Hnilo J, Marlais S, Phillips T, Potter G, Santer BD, Sperber KR, Taylor K, Williams D (1999)   An overview of the results of the Atmospheric Model Intercomparison Project (AMIP I). Bull Am Met Soc 80 , 29-55

Gillet NP, Zwiers FW, Weaver AJ, Hegerl GC, Allen MR, Stott PA   (2002) Detecting anthropogenic influence with amultimodel ensemble. Geophys. Res. Lett. 29(20) doi:10.1029/2002GL015836

Giorgi F , Mearns LO (2002) Calculation of average, uncertainty range and reliability of regional climate changes from AOGCM simulations via the "Reliability Ensemble Averaging" (REA) method. J Climate 15,   1141-1158

IPCC (2007) Summary for Policymakers. In: *Climate Change 2007: The Physical Science Basis. Contribution of Working Group I to the Fourth Assessment Report of the Intergovernmental Panel on Climate Change* [Solomon, S., D. Qin, M. Manning, Z. Chen, M. Marquis, K.B. Averyt, M.Tignor and H.L. Miller (eds.)]. Cambridge University Press, Cambridge, United Kingdom and New York, NY, USA.

Kalnay E, Kanamitsu M, Kistler R, Collins W, Deaven D,Gandin L, Iredell L, Saha S, White G, Wollen J, Zhu Y,Chelliah M, EbisuzakiW, HigginsW, Janowiak J, Mo KC, Ropelewski C,Wang J, Leetmaa A, Reynolds R, Jenne R,Joseph D (1996) The NCEP-NCAR 40-year reanalysis project. Bull Amer Meteor Soc 77, 437–471

Kang IS, Jin K, Wang B, Lau KM, Shukla J, Krishnamurty V, Shubert SD, Waliser DE, Stern WF, Kitoh A, Meehk GA, Kanamitsu M, Galin VY, Satyan V, Park CK, Liu Y (2002) Intercomparison of climatological variations of Asian summer monsoon precipitation simulated by 10 GCMs. Clim Dyn 19 , 383-395

Kripalani RH, Kulkarni A (1997) Climatic impact of El Nino / La Nina on the Indian monsoon : a new perspective. Weather 52, 39-46

Kripalani RH, Kulkarni A (1999) Climatology and variability of historical Soviet snow depth: some new perspectives in snow-Indian monsoon teleconnections. Clim Dyn 15 , 475-489

Kripalani RH, Oh J-H, Knag J-H, Sabade SS, Kulkarni A (2005) Extreme monsoons over East Asia : Possible role of Indian Ocean zonal mode. Theor Appl Climatol, 82, 81-94

Kripalani RH, Oh JH, Kulkarni A, Sabade SS, Chaudhari HS (2007a) South Asian summer monsoon precipitation variability : Coupled climate model simulations and projections under IPCC AR4. Theor Appld Climatol 90 , 133-159

Kripalani RH, Oh JH, Chaudhari HS (2007b) Response of the East Asian summer monsoon to doubled atmospheric CO2 : Coupled climate model simulations and projections under IPCC AR4. Theor Appld Climatol 87, 1-28

Krishna Kumar K, Rajagopalan B, Cane MA (1999) On the weakening relationship between the Indian monsoon and ENSO. Science 284, 2156-2159

Kulkarni A, Kripalani RH, Singh SV (1992) Classification of summer monsoon rainfall patterns over India. Int J Climatology 12, 269-280

Kulkarni A, Sabade SS, Kripalani RH (2007) Association between extreme monsoons and the dipole mode over the Indian subcontinent. Met Atmos Phys, 95, 255-268

May W (2004) Potential future changes in the Indian summer monsoon due to greenhouse warming: analysis of mechanism in a global time-slice experiment. Clim Dyn 22, 389-414

McAvaney BJ, Covey C, Joussaume, Kattsov V, Kitoh A, Ogana W, Pitman AJ, Weaver AJ, Wood RA and Zhao ZC (2001) Model Evaluation. *Climate Change 2001: The Scientific Basis. Contribution of Working Group I to the Third Assessment report of the Intergovernmental Panel on Climate Change* (Houghton JT, Y Ding, DJ Griggs, M Noguer, PJ van der Linden, X Dai, K Maskell, and CA Johnson (eds.)). Cambridge University Press, United Kingdom and New York, NY, USA, 881 pp.

Meehl GA, Boer GJ, Covey C, Latif M, Stouffer RJ (2000) The coupled model Intercomparison project (CMIP). Bull Amer Meteor Soc 81, 313-318

Meehl GA, Covey C, Delworth T, Latif M, McAvaney B, Mitchell JFB, Stouffer RJ, Taylor KE, (2007a) The WCRP CMIP3 multimodel dataset. A new era in climate change research. Bull Am Met Soc 88, 1383-1394

Meehl, G.A., T.F. Stocker, W.D. Collins, P. Friedlingstein, A.T. Gaye, J.M. Gregory, A. Kitoh, R. Knutti, J.M. Murphy, A. Noda, S.C.B. Raper,I.G. Watterson, A.J. Weaver and Z.-C. Zhao, (2007b) Global Climate Projections. In: *Climate Change 2007: The Physical Science Basis. Contribution of Working Group I to the Fourth Assessment Report of the Intergovernmental Panel on Climate Change* [Solomon, S., D. Qin, M. Manning, Z. Chen, M. Marquis, K.B. Averyt, M. Tignor and H.L. Miller (eds.)]. Cambridge University Press, Cambridge, United Kingdom and New York, NY, USA.

Rao, S., Yamagata T (2004) Abrupt termination of IndianOcean dipole events in response tointraseasonal disturbances.*Geophys. Res. Lett.,* **31,** L19306, doi:10.1029/ 2004GL020842.

Sabade SS, Kulkarni A, Kripalani RH (2009) Projected changes in South Asian summer monsoon by multi-model global warming experiments, Theor Appld Climatol, submitted

Saji NH, Goswami BN, Vinayachandran PN, Yamagata T (1999) A dipole mode in the tropical Indian Ocean. Nature, 401**,** 360–363.

Saji NH, Xie SP, Yamagata T (2006) Tropical Indian Ocean Variability in the IPCC Twentieth-Century Climate Simulations. J Climate, 19, 4397-4417

Taylor KE (2001) Summarizing multiple aspects of model performance in a single diagram. J Geophys. Res 106 : 7183-7192

Ueda H, Iwai A, Kuwako K, Hori ME (2006) Impact of anthropogenic forcing on the Asian summer monsoon as simulated by 8 GCMs. Geophys Res Let*t* 33 doi: 10.1029/2005GL025336

Xie P and Arkin PA (1997) Global precipitation: a 17-year monthly analysis based on gauge observations, satellite estimates and numerical model outputs. Bull Am Met Soc 78 : 2539-2558.

Table 1: Climate modeling groups participated in IPCC AR4, their IPCC identification and their key reference. The simplified abbreviations will be used throughout the text to refer to a particular model. Models used for future projections are highlighted. Models for which data are not available are shown in italics

Ser No	IPCC ID	Simplified Abbreviation	Originating Group	Key Reference
1	BCC-CM1	Bcc	Beijing Climate Center China	Dong , 2001
2	**BCCR-BCM.0**	**bccr/bcr**	Bjerkness Center for Climate Research, Norway Norway	Furevik et al 2003
3	**CGCM3.1(T47)**	**cgcm/ccm**	Canadian Centre for Climate Modeling and Analysis , Canada	Flato et al 2000
4	**CGCM3.1(T63)**	**cgcm2/ccm2**	Canadian Centre for Climate Modeling and Analysis, Canada	Flato et al 2004
5	**CNRM-CM3**	**cnrm/cnr**	Meteo-France/Center National de Recherches Meteorologiques, France	Salas-Melia et al 2005
6	CSIRO-MK3.0	Csiro/csr	CSIRO Atmospheric Research, Australia	Gordon et al 2002
7	*CSIRO-MK3_5*	*csr35*	*CSIRO Atmospheric Research, Australia*	*Mark Collier et al 2005*
8	GFDL-CM2.0	gfdl0/gf0	US Dept of Commerce NOAA/ GFDL, USA	Delworth et al 2006
9	GFDL-CM2.1	gfdl1/gf1	US Dept of Commerce NOAA/ GFDL , USA	Delworth et al 2006
10	GISS-AOM	gissagia	NASA/GISS, USA	Russel et al 1995
11	GISS-EH	Gissh/gih	NASA/GISS, USA	Schmidt et al 2005
12	GISS-ER	Gissr/gir	NASA/GISS, USA	Schmidt et al 2005
13	*FGOALS-g1.0*	*Fgoal/iap*	*LASG/ Institute of Atmospheric Physics, China*	*Yu et al 2004*
14	**INM-CM3.0_0**	**inmcm/inm**	Institute of Numerical Mathematics, Russia	Diansky & Volodon 2002
15	IPSL-CM4	Ipsl/ips	Institut Pierre Simon Laplace, France	Marti et al 2005
16	*INGV-SXG*	*Ingv/ing*	*Instituto Nazionale di Geofisica e vulcanologia, Italy*	*Guialdi et al 2006*

17	**MIROC3.2(hires)**	**miroch/mih**	Center for Climate System Research (The University of Tokyo) National Institute for Environmental Studies and Frontier Research Center for Global Change (JAMSTEC) Japan	K-1 Model Developers 2004
18	**MIROC3.2 (medres)**	**mirocm/mim**	Center for Climate System Research (The University of Tokyo) National Institute for Environmental Studies and Frontier Research Center for Global Change (JAMSTEC)Japan	K-1 Model Developers 2004
19	**ECHO-G**	**eco**	Meteorological Institute of University of Bonn, METRI of KMA	Legutke and Voss 1999
20	**ECHAM5/MPI-OM**	**echam/ech**	Max Planck Institute for Meteorology,Germany	Jungclaus et al 2005
21	MRI-CGCM2.3.2	mri	Meteorological Research Institute,Japan	Yukimoto & Noda 2002
22	CCSM3	ccsm/ncc	NCAR, USA	Collins et al 2006
23	PCM	Pcm/ncp	NCAR, USA	Washington et al 2000
24	**UKMO-HadCM3**	**ukmoc/ukc**	Hadley Center for Climate Prediction and Research/Meteorological Office, UK	Jones et al 2004
25	UKMO-Hadgem1	Ukmog/ukg	Hadley Center for Climate Prediction and Research/Meteorological Office, UK	Johns et al 2004

Table 2 : Characteristics of the climate models: Approximate Gaussian grid atmospheric resolution (lon x lat), Convection schemes used (AS=Arakawa-Schubert, RAS=Relaxed Arakawa-Schubert, MF=Mass flux-based, MC=Moist Convection Adjustment) Flux corrections at the Ocean-Atmosphere interface (N=None, H=Heat, W=Water, M=Momentum). A dash (-) indicates information not available. Models for which data are not available are shown in italics.

No.	Model Acronym	Covection Scheme	Flux Correction	Resolution Gaussian grid	Period '20c3m'
1	bcc_cm1	-	-	2.8125 x 2.8125	1850-1999
2	bccr_bcm2_0	MF	N	2.8125 x 2.8125	1950-1999
3	cccma_cgcm3_1	MC	HW	3.75 x 3.75	1850-2000
4	cccma_cgcm3_1_t63	MC	HW	2.8125 x 2.8125	1850-2000
5	cnrm_cm3	MF	N	2.8125 x 2.8125	1860-1999
6	csiro_mk3	MC	N	1.875 x 1.875	1871-2000
7	*csiro_mk3_5*	*MC*	*N*	*1.875 x 1.875*	*1871-2000*
8	gfdl_cm2_0	RAS	N	2.5 x 2	1861-2000
9	gfdl_cm2_1	RAS	N	2.5 x 2	1861-2000
10	giss_aom	MF	N	4 x 3	1850-2000
11	giss_model_e_h	MF	N	5 x 4	1880-1999
12	giss_model_e_r	MF	N	5 x 4	1880-2003
13	*iap_fgoals1_0_g*	*MF*	*N*	*2.8125 x 3*	*1850-1999*
14	*ingv_echam4*	*MF*	*N*	*1.125 x 1. 125*	*1870-2000*
15	inmcm3_0	MC	W	5 x 4	1871-2000
16	ipsl_cm4	MC	N	3.75 x 2.5	1860-2000
17	miroc3_2_hires	AS	N	1.125 x 1.125	1900-2000
18	miroc3_2_medres	AS	N	2.8125 x 2.8125	1850-2000
19	miub echo_g	MF	N	3.75 x 3.75	1850-1999
20	mpi_echam5	MF	N	1.875 x 1.875	1860-2100
21	mri_cgcm2_3_2a	AS	HWM	2.8125 x 2.8125	1851-2000
22	ncar_ccsm3_0	AS	N	1.40625 x1.40625	1870-1999
23	ncar_pcm1	AS	N	2.8125 x 2.8125	1890-1999
24	ukmo_hadcm3	MF	N	3.75 x 2.4657	1860-1999
25	ukmo_hadgem1	MF	N	1.875 x 1.24	1860-1999
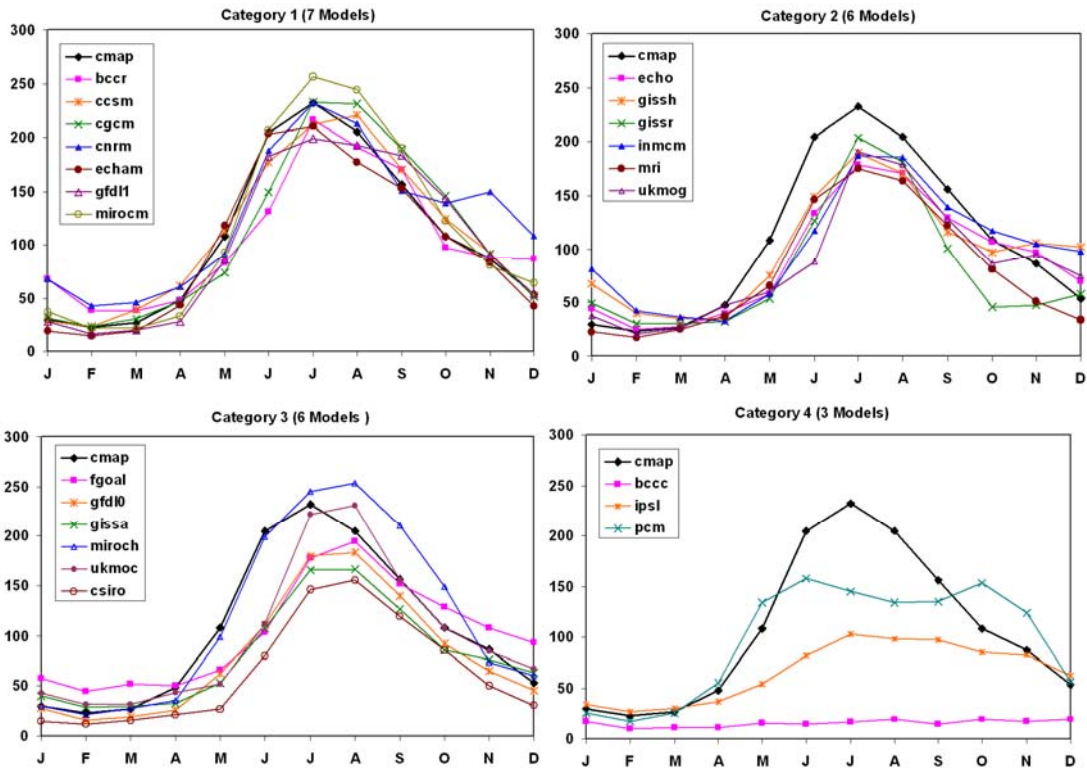
Fig 1 : Average monthly rainfall (mm) for the observed (cmap) and simulated by the 22 coupled models depicting the annual cycle (J = January – – – – – D-=December) over the south Asian region. Category 1: Models simulating shape and magnitude well; Category 2: models simulating shape well but underestimating magnitude; Category 3: models simulating a shift in peak precipitation by a month; Category 4: models unable to simulate the annual cycle properly. Models are identified by their acronyms
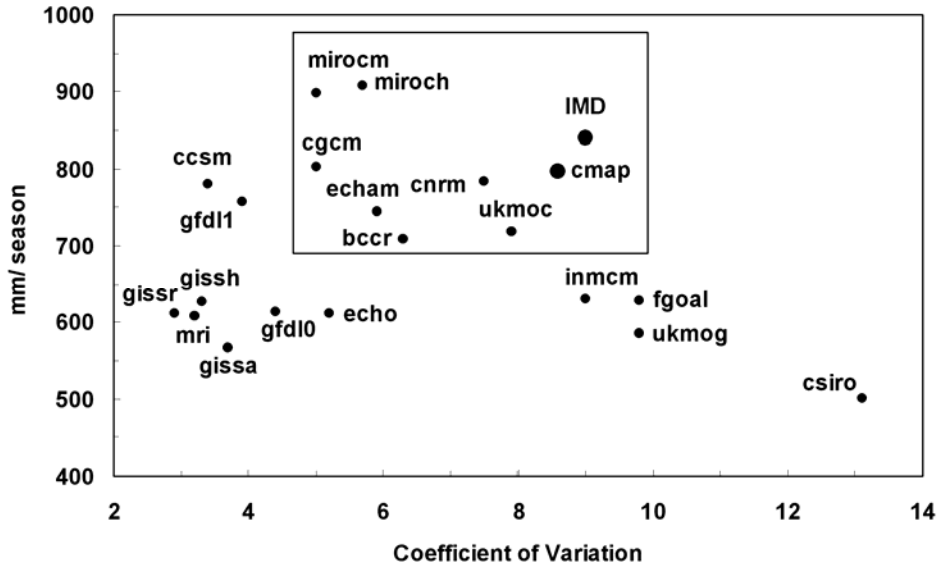
Fig 2 : Scatter plot of the mean seasonal (JJAS) rainfall in mm and the coefficient of variation (in %) for the 19 coupled models. Each dot represents the corresponding values for each model, identified by their acronyms. Observed values are depicted as cmap and IMD (see text). The models in the rectangular box are identified for projections
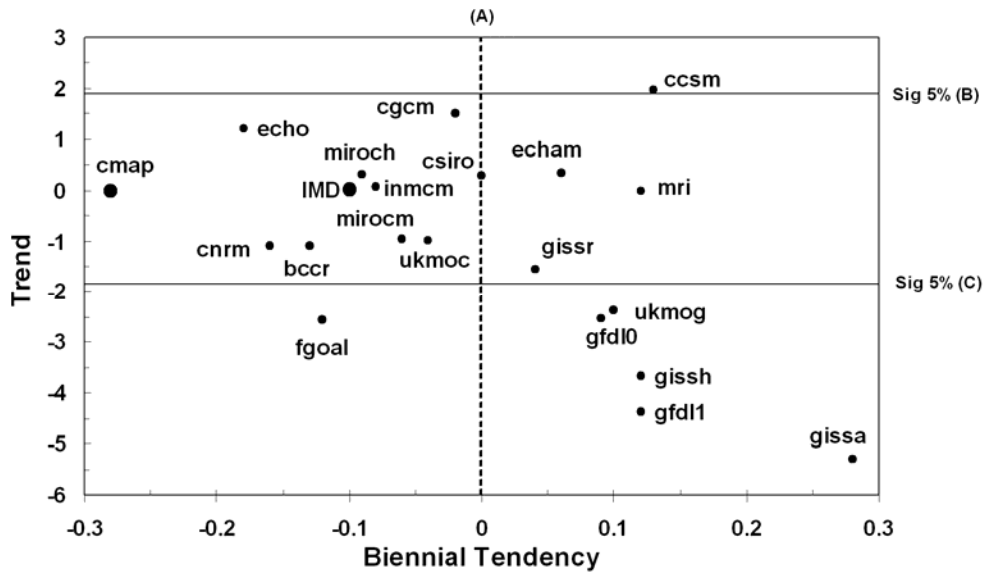
Fig 3 : Same as Fig. 3 but for the trend (Mann-Kendall statistic) and biennial tendency (lag-1 autocorrelation). Models on the left (right) of vertical dashed line A reflect (do not reflect) biennial tendency. Horizontal lines B and C indicate the trend values at 5% significance level. Models lying between the lines B and C show no trends. Models are identified by their acronyms. Values based on cmap and IMD are also indicated

22
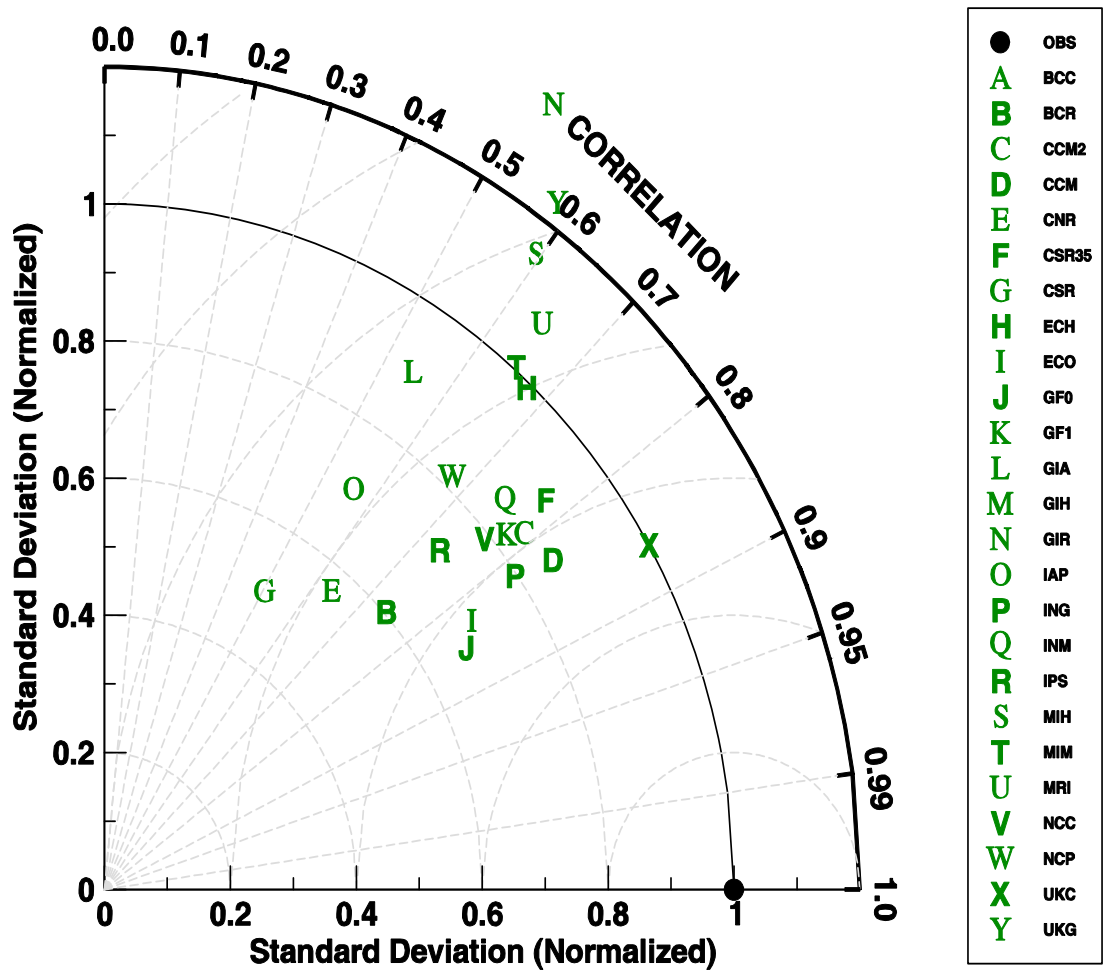
Fig 4 : Taylor diagram for seasonal (June through September) mean monsoon rainfall over South Asia
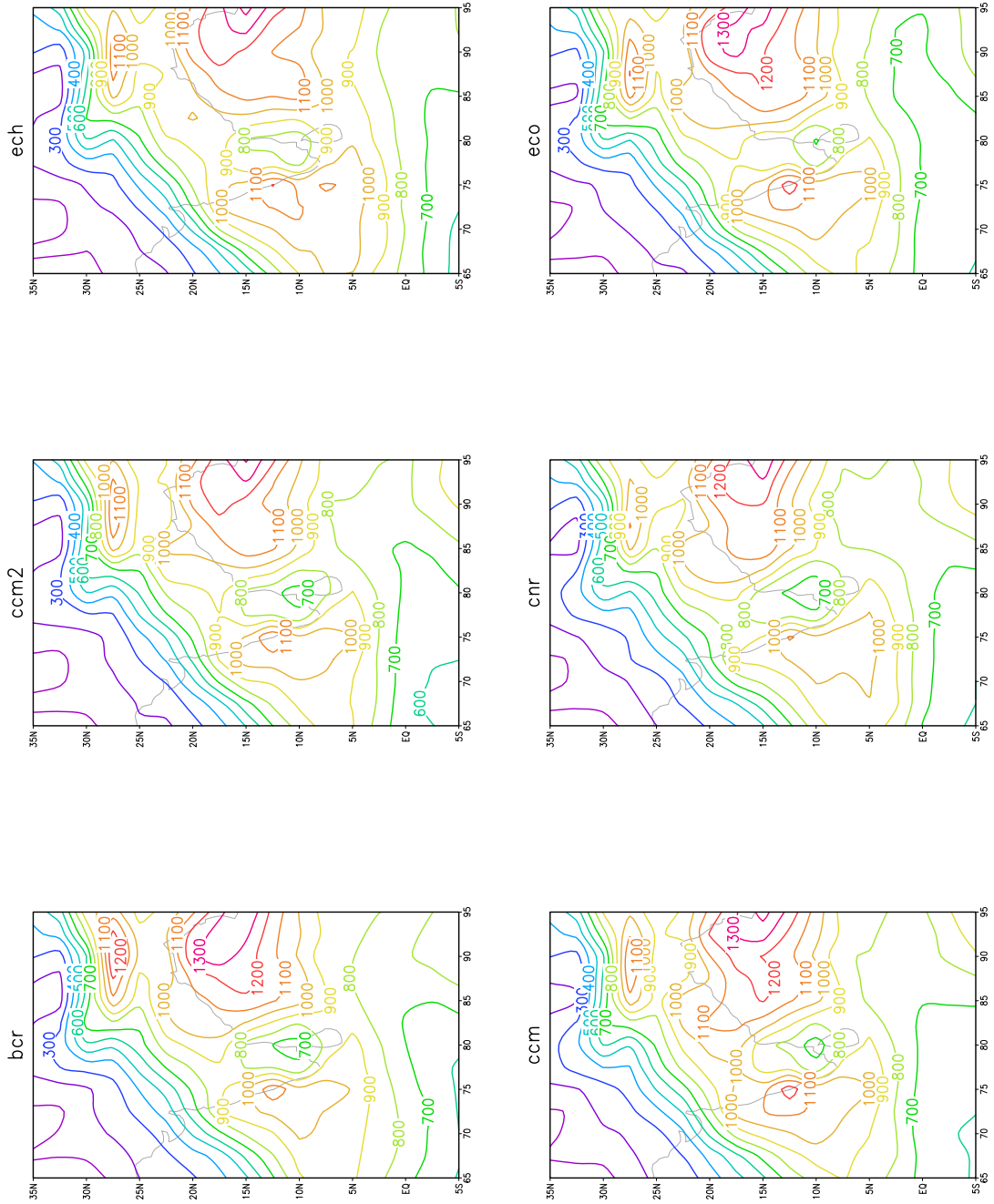
Fig 5 : Seasonal mean rainfall (mm) simulated by selected 10 models , their MME and the observed rainfall pattern for CMAP over South Asian region
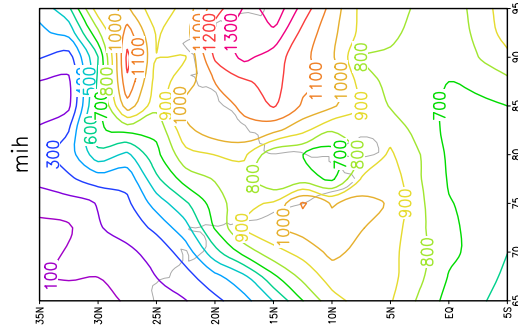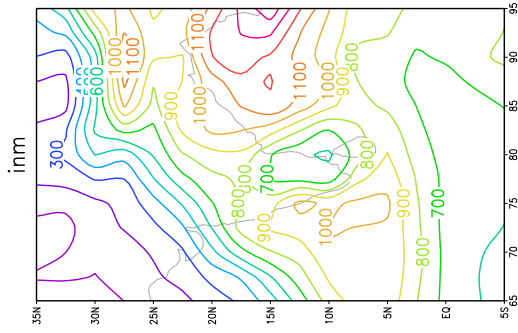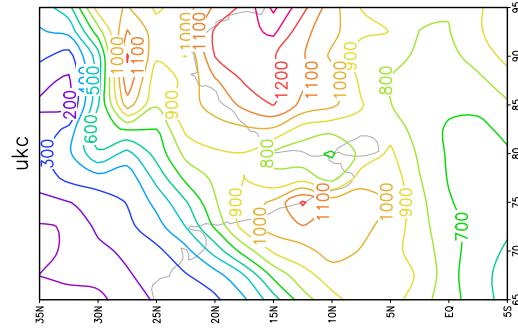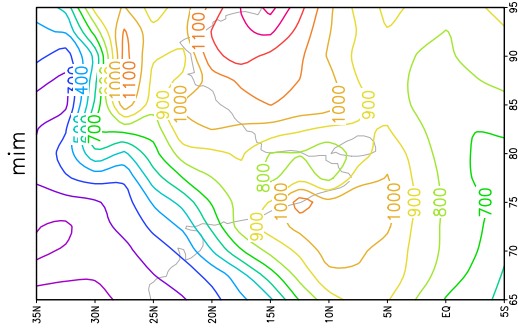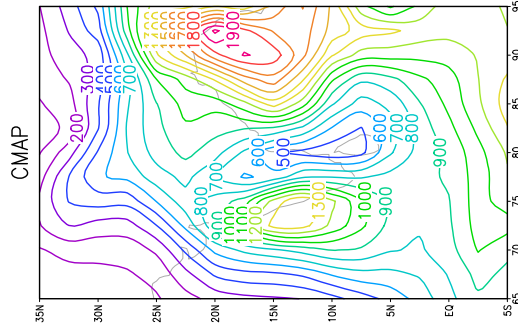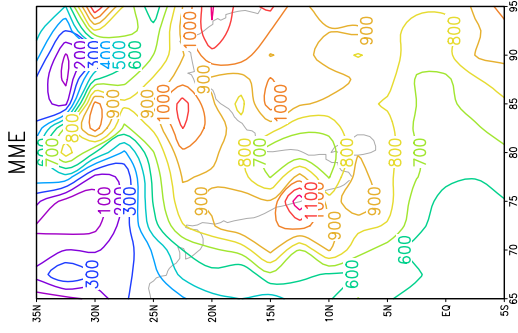
Fig 5 (Contd)
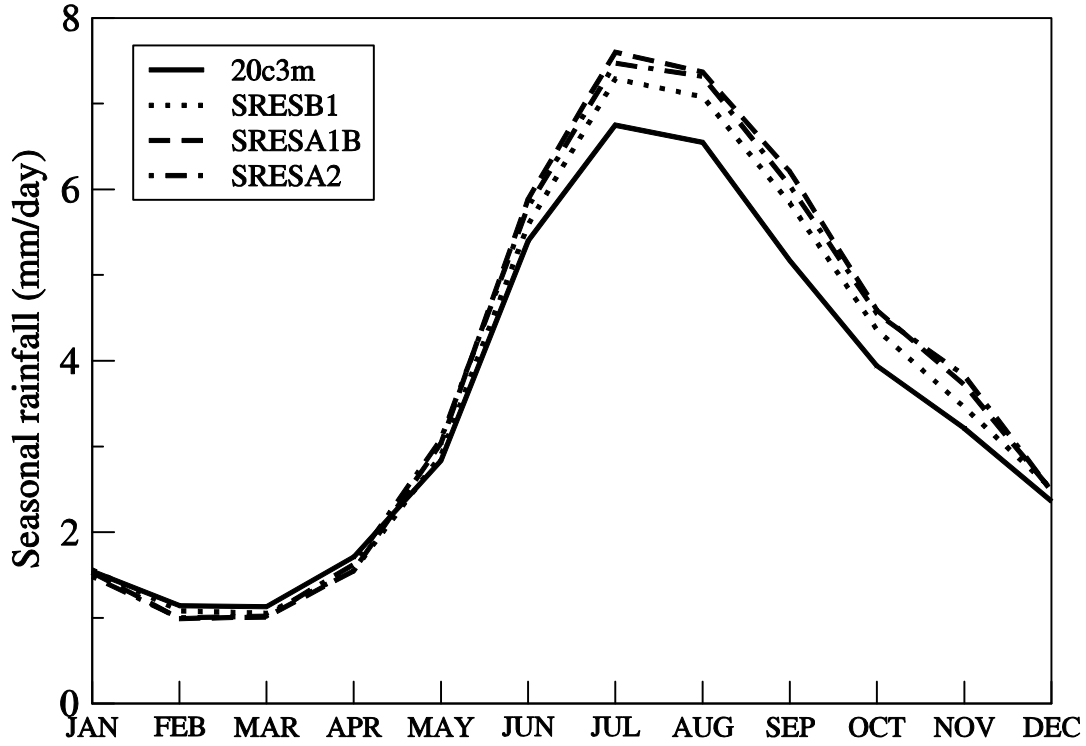
Fig 6 : MME of monthly average rainfall (mm/day) for 20c3m (1981-2000) and SRES
B1, A1B and A2 (2081-2100)
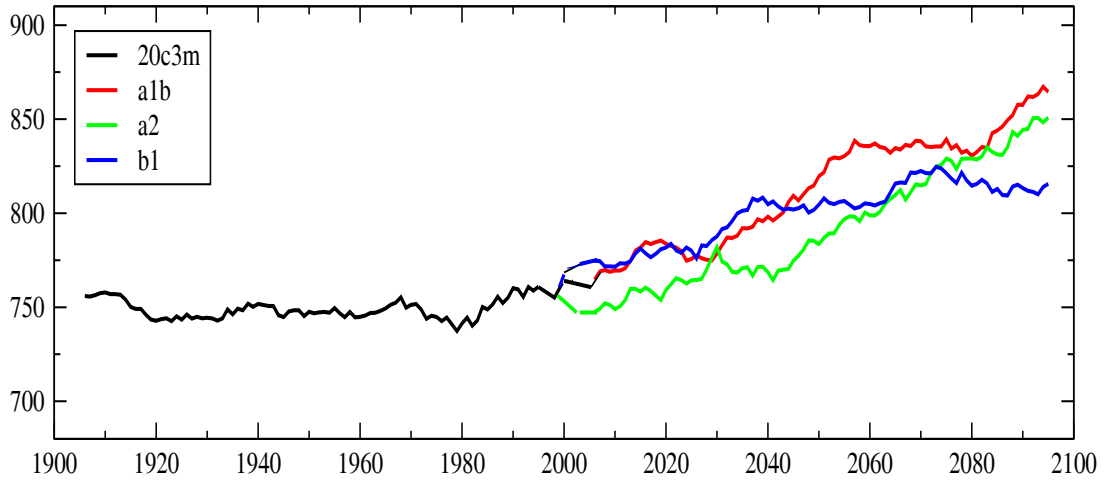
**Fig 7** : 11-year running average of MME time series of seasonal monsoon rainfall (mm)
for 20c3m (1901-2000) and SRES B1, A1B and A2 (2001-2100)

26
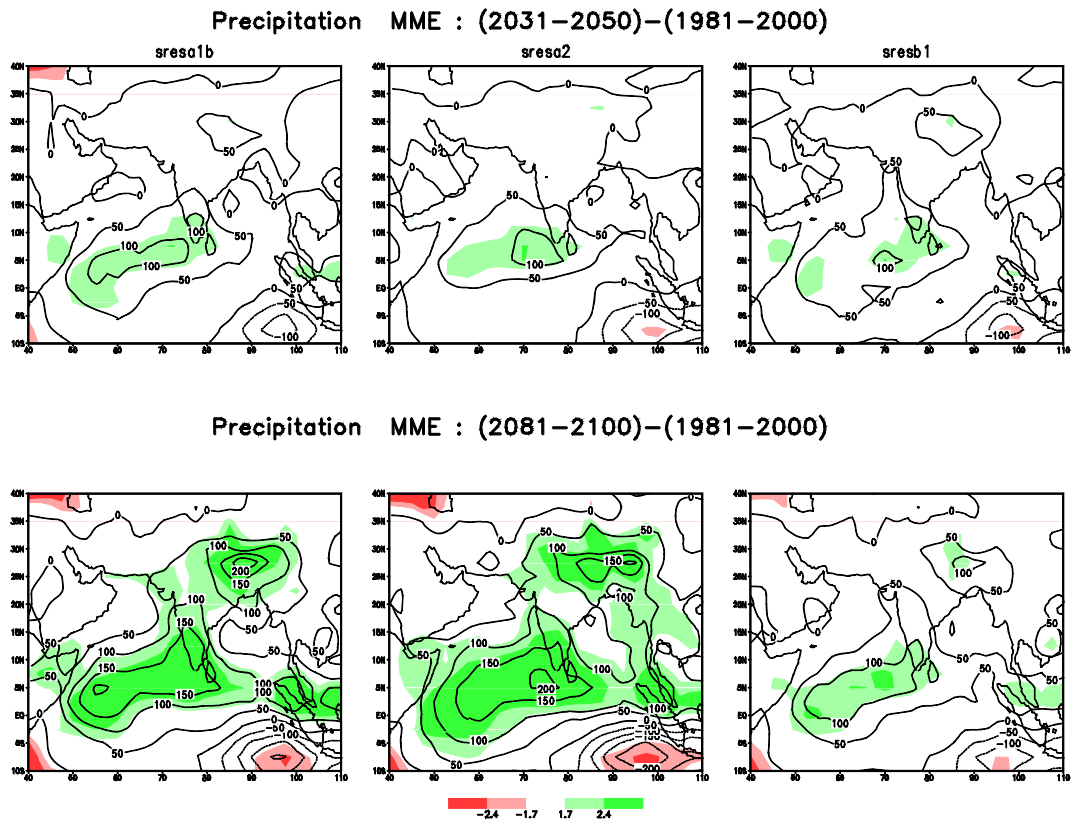
Fig 8 : MME of change in seasonal precipitation amount (mm) in SRES A1B , A2 and B1 with respect to 20c3m (1981-2000) in two time slices 2031-2050 (top panels) and 2081 -2100 (bottom panels). The shading denotes the significant difference at 5% and 1% level.

May SLP   MME : (2031-2050)-(1981-2000)
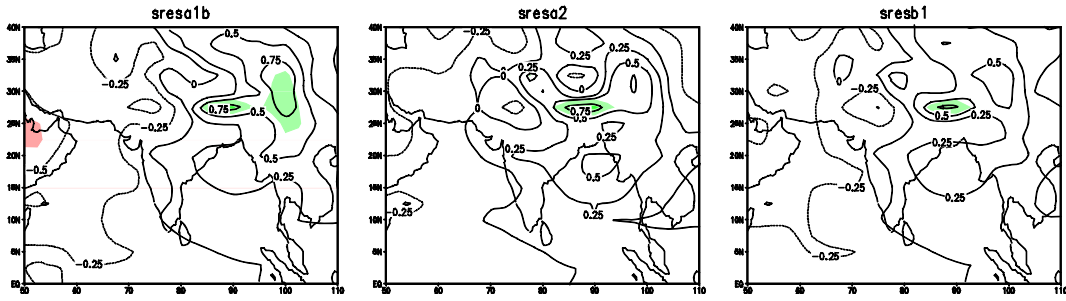
May SLP   MME : (2081-2100)-(1981-2000)
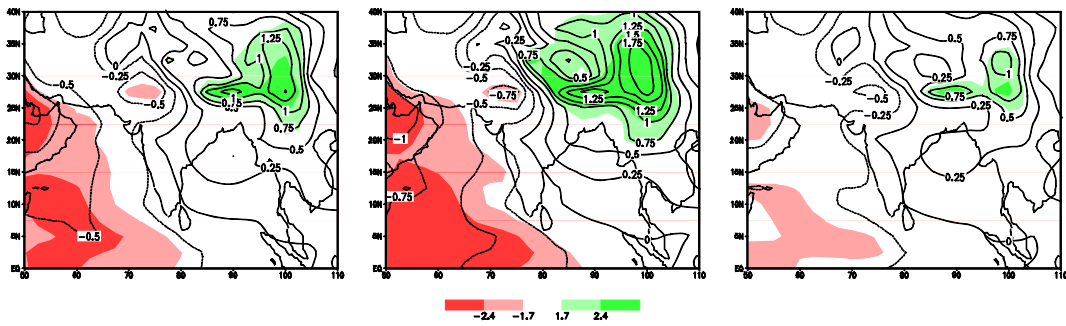
Fig 9 : Same as Fig 8 but for sea level pressure in May

Change in circulation MME : (2031-2050)-(1981-2000)

Change in circulation MME : (2081-2100)-(1981-2000)
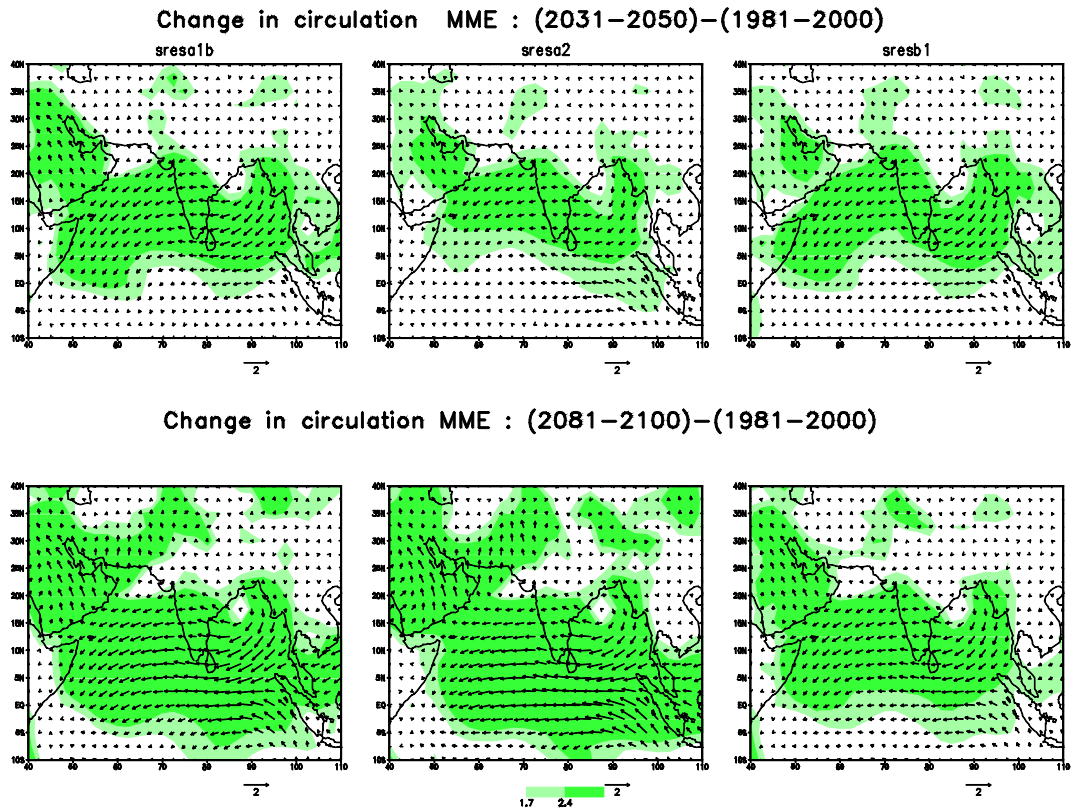
Fig 10 : Same as Fig 9 but for 850 hPa vector winds in JJAS

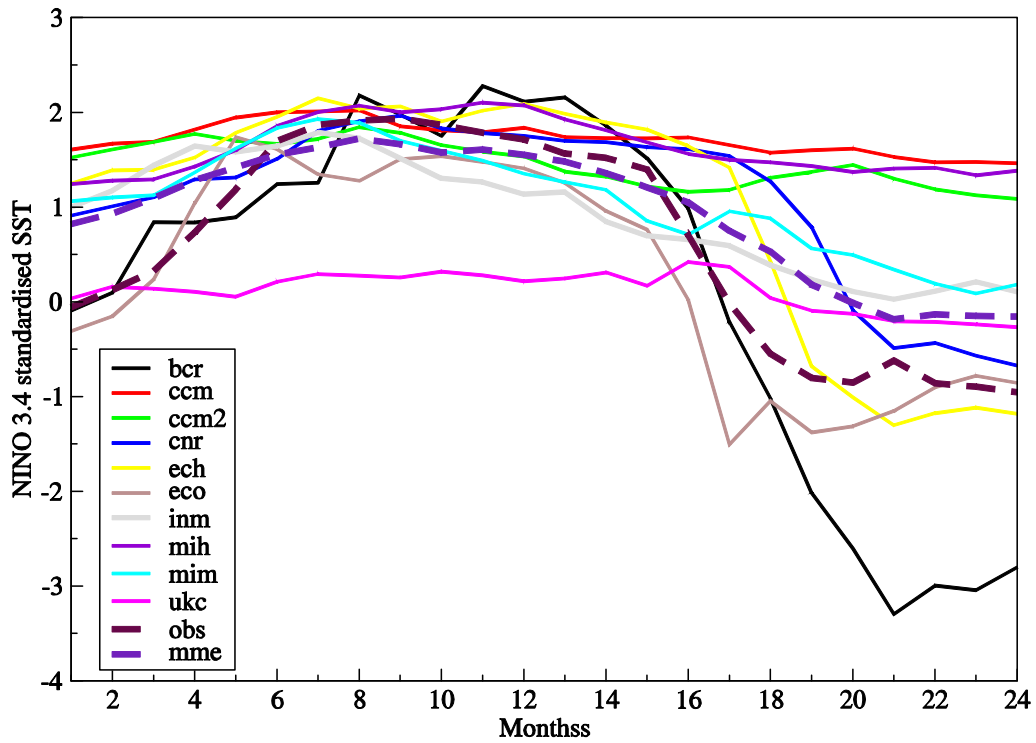**Winter Snow MME (2031-2050)-(1981-2000)**

Winter Snow MME (2081-2100)-(1981-2000)
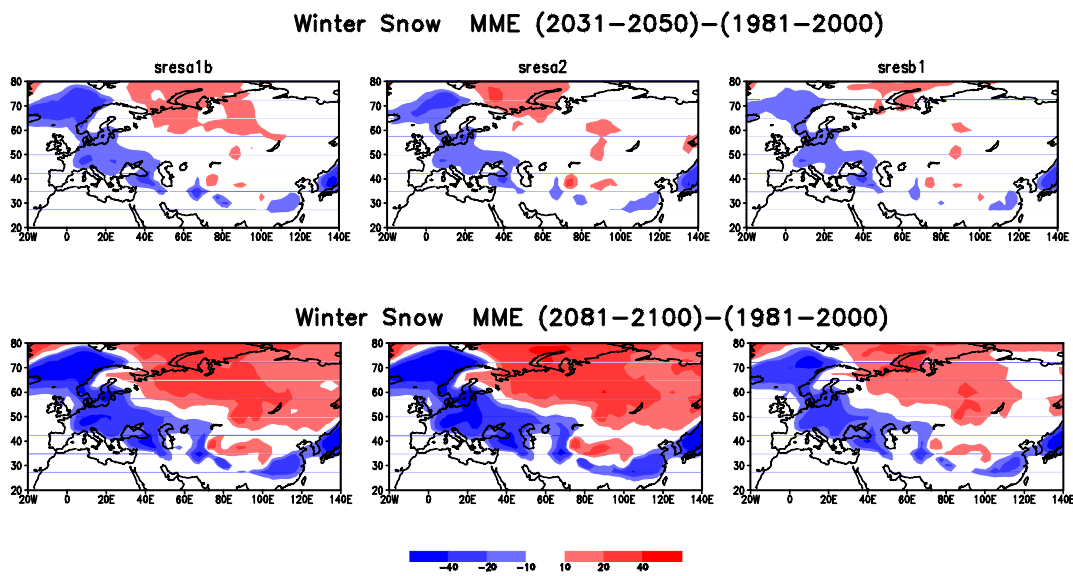
**Fig 11** : MME of change in snow cover (mm) in winter (Dec-Jan-Feb)
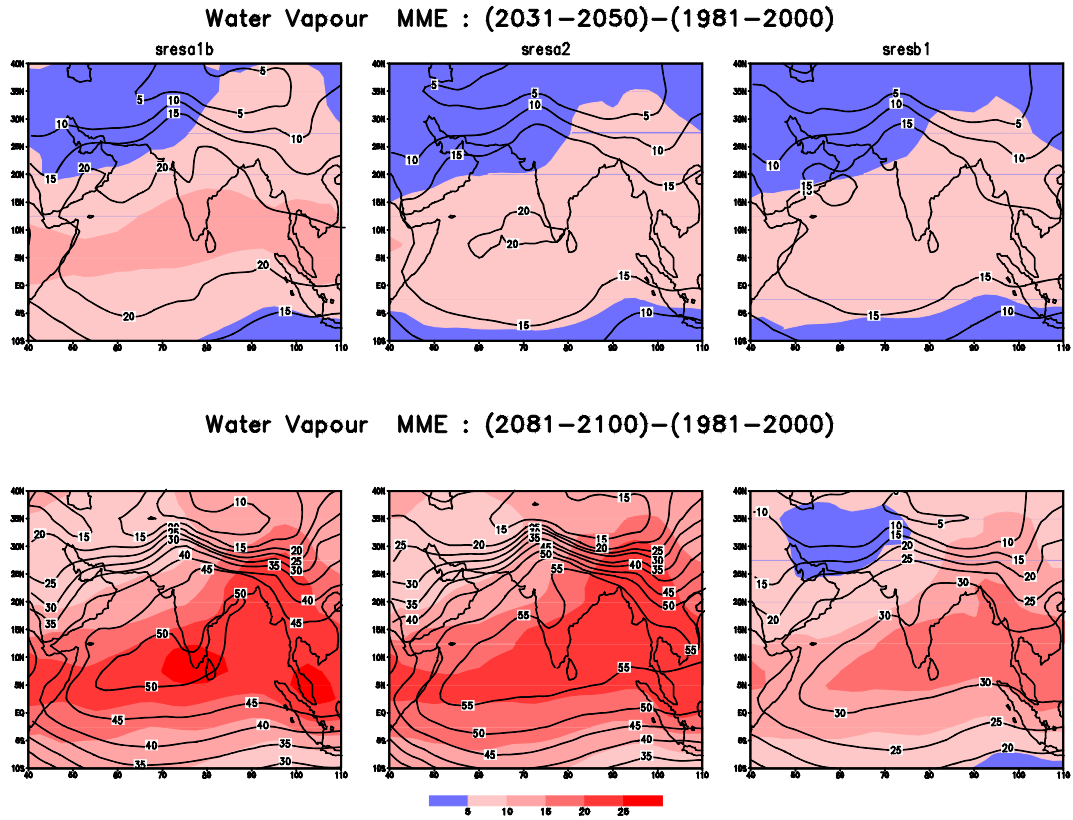
Fig 12: MME of change in water vapour content in summer monsoon season

Fig 13 : Monthly temporal evolution of standardized SSTs over NINO3.4 region from
10 models, their MME and observed HADISST data. The composites are based
on strong El Nino events (standardized JJAS SSTs > +1.0 over NINO3.4 region)
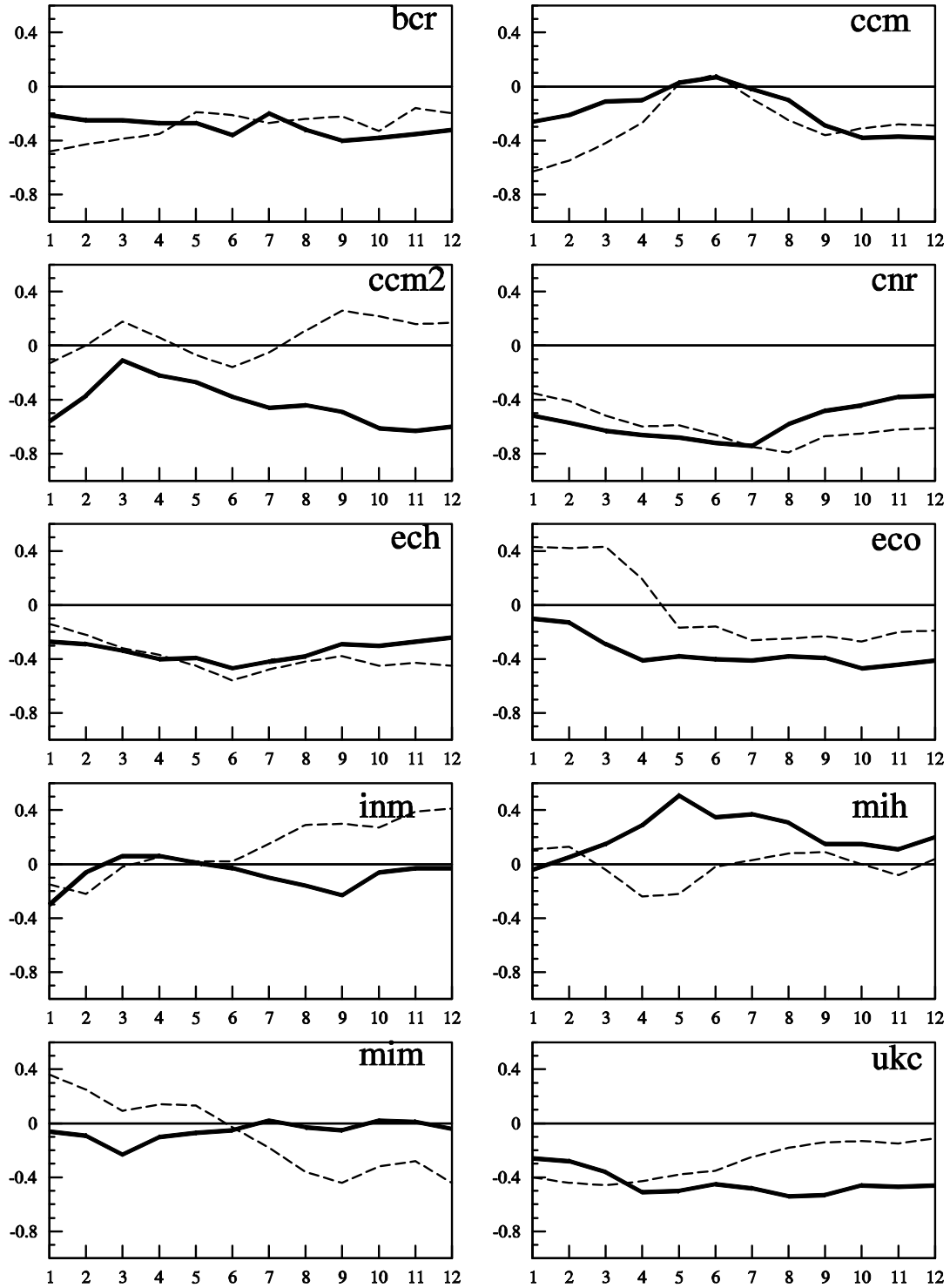
Fig 14 : The relationship between monthly SSTs over NINO3.4 region and seasonal monsoon rainfall over South Asia simulated by 10 models in 20c3m in two time slices 1961 -1980 (solid line) and 1981-2000((dashed line)
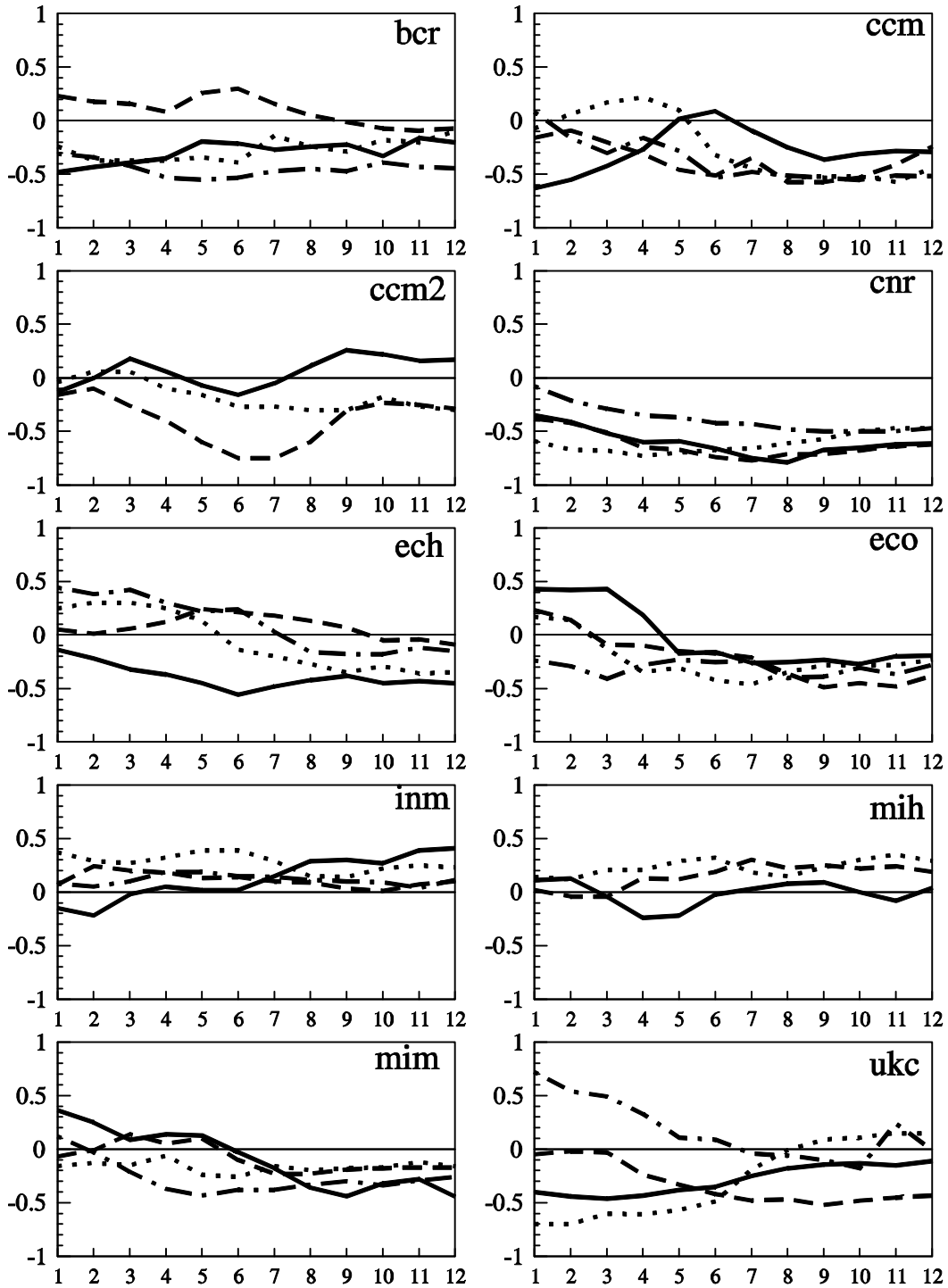
Fig 15 : Same as Fig 14 but for 20c3m (1981-2000, solid line), SRES B1 (dotted line), A1B (dashed line) and B2 (dash-dot line) for 2081-2100
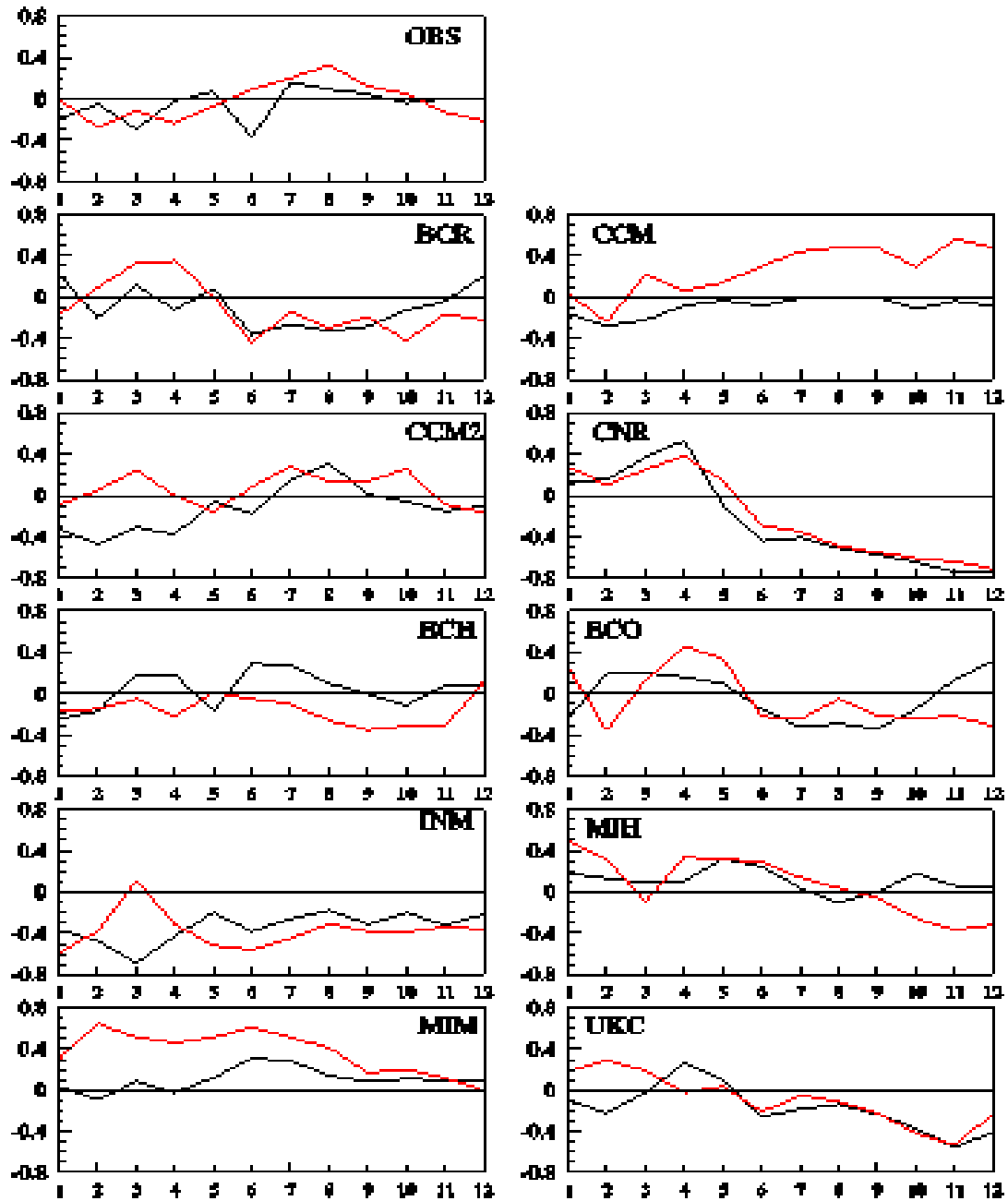
Fig 16 : Observed and simulated correlations between monthly Dipole Mode Index and seasonal monsoon rainfall for two time slices 1961-1980 (black) and 1981-2000(red)